IGARSS 2020 - 2020 IEEE International Geoscience and Remote Sensing Symposium | 978-1-7281-6374-1/20/$31.00 ©2020 IEEE | DOI: 10.1109/IGARSS39084.2020.9323926

SPECTRAL-SPATIAL WEIGHTED SPARSE NONNEGATIVE TENSOR FACTORIZATION FOR HYPERSPECTRAL UNMIXING

Shaoquan Zhang[1], *Guorong Zhang*[1], *Chengzhi Deng**[1], *Jun Li*[2], *Shengqian Wang*[1], *Jun Wang*[1], *Antonio Plaza*[3]

[1]Jiangxi Province Key Laboratory of Water Information Cooperative Sensing and Intelligent Processing, Nanchang Institute of Technology, Nanchang, 330099, China.
[2]Guangdong Provincial Key Laboratory of Urbanization and Geo-simulation, School of Geography and Planning, Sun Yat-sen University, Guangzhou, 510275, China.
[3]Hyperspectral Computing Laboratory, Department of Technology of Computers and Communications, Escuela Politécnica, University of Extremadura, Cáceres, E-10003, Spain.

ABSTRACT

Hyperspectral unmixing aims to decompose a hyperspectral image (HSI) into a collection of constituent materials, or endmembers, and their corresponding abundance fractions. Recently, nonnegative tensor factorization (NTF)-based spectral unmixing methods have attracted significant attention owing to their outstanding performance when representing an HSI without any information loss. However, tensor factorization-based HSI methods do not fully exploit the spatial contextual information present in the scene. Besides, these approaches are sensitive to low signal-to-noise ratio (SNR) in HSIs. To address this limitation, we propose a new spectral-spatial weighted sparse nonnegative tensor factorization (SSWNTF) method to preserve the spatial details in the abundance maps via the spectral and spatial weighting factors. Our experiments with simulated data sets certified that the proposed method outperforms other advanced methods.

Index Terms— Hyperspectral unmixing, blind source separation, nonnegative tensor factorization, spatial information.

1. INTRODUCTION

Due to insufficient spatial resolution and spatial complexity, pixels in remotely sensed hyperspectral images (HSIs) are likely to be formed by a mixture of pure spectral constituents (*endmembers*) rather than a single substance [1]. Spectral unmixing, which estimates the fractional abundances of the pure spectral signatures or endmembers in each mixed pixel, was proposed to deal with the mixing problem [2].

This work was supported in part by the Science and Technology Project of Jiangxi Provincial Department of Education under Grant GJJ180962, in part by Jiangxi Provincial Natural Science Foundation under Grant 20192BAB217003, in part by National Natural Science Foundation of China under Grants 61901208, 61865012, 61771496, 61661033, in part by Jiangxi Provincial Key Research and Development Program of China under Grant 20181ACG70022, in part by FEDER and Junta de Extremadura (GR18060).
(Corresponding Author: Chengzhi Deng, dengchengzhi@126.com)

Linear unmixing techniques can be classified into geometrical [3] and statistical-based [4]. The former exploits the fact that the spectral vectors are in a simplex whose vertices correspond to the endmembers, whereas the latter category addresses spectral unmixing as an inference problem [1]. For the geometrical-based methods, they usually assume that pure pixels exist, i.e., they contain only one type of material. However, in many cases, the existence of pure pixels in an image cannot be guaranteed. Here, we focus on the statistical approach to spectral unmixing.

From the statistical point of view, hyperspectral unmixing can be treated as a blind source separation (BSS) problem. Nonnegative matrix factorization (NMF)-based unmixing [5, 6] is a classic method in statistics that not only provides a fully unsupervised procedure (without the pure pixel assumption), but is also able to simultaneously determine the endmember signatures and corresponding fractional abundances. However, due to the fact that the cost function of the standard NMF model is nonconvex, there may exist many local optimal solutions. To alleviate this situation, researchers have introduced a series of additional constraints into the standard NMF model. On the one hand, some methods impose constraints on the endmembers themselves. The minimum volume constrained nonnegative matrix factorization (MVC-NMF) [7] is one of the most representative of such methods. On the other hand, other methods impose constraints on the abundances, such as $L_{1/2}$-NMF [8], the graph-regularized $L_{1/2}$-NMF (GLNMF) [9], and the total variation regularized reweighted sparse NMF (TV-RSNMF) [10].

Even though these constrained NMF methods offer promising performance, under a matrix factorization framework information loss is unavoidable when unfolding a 3-D HSI into a 2-D matrix form. Compared to matrices, tensors [11] offer a more natural representation of HSI cubes which characterizes two spatial dimensions and one spectral dimension. Tensor decompositions have been widely applied for HSI feature extraction, denoising and target de-

tection [12]. Recently, the matrix-vector nonnegative tensor factorization (MV-NTF) [13] unmixing method based on block-term decomposition (BTD) has been proposed, which has obtained encouraging unmixing results. The introduction of MV-NTF opened new avenues and brought new insights into the concept of NTF unmixing. However, in practical applications, the results of tensor decomposition are usually unstable due to its sensitivity to low SNR. Furthermore, the BTD takes the tensor data as a whole and ignores the detailed spatial structure information contained in the scene.

Inspired by the success of weighted ℓ_1 minimization in sparse signal recovery [14], in this paper we proposed a new spectral-spatial weighted sparse nonnegative tensor factorization (SSWNTF) hyperspectral unmixing method. The proposed SSWNTF method aims at simultaneously exploiting the sparsity as well as the spatial smoothness of fractional abundances. On the one hand, the spatial weighting factor is used to promote piecewise smoothness in abundance maps and alleviate the drawbacks of the NTF-based methods in noisy scenarios. On the other hand, the spectral weighting factor is used to enhance the sparsity of the solution. In the implementation of SSWNTF, an augmented multiplicative update scheme is proposed to solve the optimization problem.

The remainder of the paper is organized as follows. In Section 2, we briefly describe some related works. Section 3 describes the proposed SSWNTF method in detail. Section 4 presents the experimental results with simulated hyperspectral scenes. Finally, section 5 concludes the paper with some remarks and hints at plausible future research lines.

2. RELATED WORKS

Let $\mathbf{X} \in \mathbb{R}^{K\times N}$ denote a hyperspectral image, where N is the number of pixel vectors and K is the number of bands. The linear mixture model can be expressed as

$$\mathbf{X} = \mathbf{AS} + \mathbf{E} \tag{1}$$

where $\mathbf{A} \in \mathbb{R}^{K\times R}$ represents a matrix containing R endmembers. $\mathbf{S} \in \mathbb{R}^{R\times N}$ denotes the abundance maps. $\mathbf{E} \in \mathbb{R}^{K\times N}$ is the additive noisy matrix. Generally, the abundance matrix $\mathbf{S}$ needs to satisfy two constraints, i.e. the abundance nonnegative constraint (ANC) and the abundance sum-to-one constraint (ASC).

The MV-NTF model [13] factorizes the observed 3-D HSI into the sum of R component tensors, where each one is the outer product of a rank L matrix and a vector, representing abundances and endmembers, respectively. It can be formulated as

$$\chi = \sum_{r=1}^{R} \mathbf{A}_r\mathbf{B}_r^T \circ \mathbf{c}_r + \mathcal{N} = \sum_{r=1}^{R} \mathbf{E}_r \circ \mathbf{c}_r + \mathcal{N} \quad \text{s.t.:}\mathbf{A},\mathbf{B},\mathbf{C} \geq 0 \tag{2}$$

where $\chi \in \mathbb{R}^{I\times J\times K}$ denotes the observed 3-D HSI with $I \times J$ pixels and K-bands. $\mathbf{E}_r \in \mathbb{R}^{I\times J}$ represents the abundance map of the r-th endmember, which is approximately represented by two rank L matrices $\mathbf{A}_r$ and $\mathbf{B}_r$. $\mathbf{c}_r$ is the r-th endmember. $\mathcal{N}$ denotes the additive noisy tensor, $\circ$ denotes the out-product. Taking the ASC into account, the solution of (2) becomes minimizing the reconstruction error between χ and its R components tensors, which is represented by

$$\min_{\mathbf{A},\mathbf{B},\mathbf{C}} \left\| \chi - \sum_{r=1}^{R} \mathbf{A}_r\mathbf{B}_r^T \circ \mathbf{c}_r \right\|_F^2 + \frac{\delta}{2}\left\|\mathbf{AB}_r^T - \mathbf{1}_{I\times J}\right\|_F^2 \quad \text{s.t.:}\mathbf{A},\mathbf{B},\mathbf{C} \geq 0 \tag{3}$$

where $\mathbf{1}_{I\times J}$ is a matrix of all-ones, $\mathbf{A} = [\mathbf{A}_1, \ldots, \mathbf{A}_R]$, $\mathbf{B} = [\mathbf{B}_1, \ldots, \mathbf{B}_R]$, $\mathbf{C} = [\mathbf{c}_1, \ldots, \mathbf{c}_R]$, the operators $\|\cdot\|_F$ denotes the Frobenius norm, δ balances the tradeoff between the reconstruction error and sum-to-one constraint.

3. PROPOSED METHOD

In order to exploit the spatial information more efficiently and protect the outcome of tensor decomposition under low SNR conditions, we develop a new method called SSWNTF for hyperspectral unmixing. Note that in order to avoid trivial solutions, we make $\sum_{r=1}^{R}(\mathbf{A}_r\mathbf{B}_r^T)$ equal to one. It is obvious that the $\sum_{r=1}^{R}(\mathbf{A}_r\mathbf{B}_r^T)$ is equal to $\mathbf{AB}^T$. The model of SSWNTF can be written as

$$\min_{\mathbf{A},\mathbf{B},\mathbf{C}} \left\| \chi - \sum_{r=1}^{R} \mathbf{A}_r\mathbf{B}_r^T \circ \mathbf{c}_r \right\|_F^2 + \frac{\delta}{2}\left\|\mathbf{AB}^T - \mathbf{1}_{I\times J}\right\|_F^2 + \lambda\sum_{r=1}^{R}\left\|(\mathbf{W}_r^{spe}\mathbf{W}_r^{spa}) \odot (\mathbf{A}_r\mathbf{B}_r^T)\right\|_1 \quad \text{s.t.}\mathbf{A},\mathbf{B},\mathbf{C} \geq 0 \tag{4}$$

where $\odot$ denotes element-wise multiplication, λ is a regularization parameter and $\delta \in \mathbb{R}^+$ balances the tradeoff between the reconstruction error and sum-to-one constraint.

For the spectral weighting factor $\mathbf{W}^{spe} \in \mathbb{R}^{R\times R}$, relying on the success of [15], we adopt row collaborativity to enforce joint sparsity among all the pixels. Let $\mathbf{S} = \mathbf{A}_r\mathbf{B}_r^T$ denote the abundance matrix. In detail, at iteration $t+1$, it can be updated as

$$\mathbf{W}^{spe,t+1} = \text{diag}[\frac{1}{||\mathbf{S}^t(1,:)||_2 + \varepsilon} \cdots \frac{1}{||\mathbf{S}^t(R,:)||_2 + \varepsilon}], \tag{5}$$

where $\mathbf{S}^t(R,:)$ denotes the R-th row in the abundance matrix at the t-th iteration, and ε is a small positive value.

Similar to the spatial weighting factor in S^{2}WSU [14], the $\mathbf{W}^{spa} \in \mathbb{R}^{R\times N}$ is used to promote piecewise smoothness in abundance maps. Let $w^{spa,t+1}$ be the element of the i-th ($i = 1, \ldots, R$) line and j-th ($j = 1, \ldots, N$) row in $\mathbf{W}^{spa}$

at iteration $t+1$. We incorporate the spatial neighborhood information as follows

$$w_{ij}^{spa,t+1} = \frac{1}{f_{h\in\mathcal{N}(j)}(s_{ij}^t)+\varepsilon}, \tag{6}$$

where $\mathcal{N}(j)$ denotes the neighboring set for element s_{ij} and $f(\cdot)$ is a function explicitly exploiting the spatial correlations through the neighborhood system. Here, the neighboring coverage and importance are used to incorporate the spatial correlation as follows

$$f(s_{ij}) = \frac{\sum_{h\in\mathcal{N}(j)} \epsilon_{ih} s_{ih}}{\sum_{h\in\mathcal{N}(j)} \epsilon_{ih}}, \tag{7}$$

where ϵ represents the neighborhood importance. For simplicity, we consider the 8-connected (3×3 window) for algorithm design and experiments. With respect to the neighboring importance, for any two entries i and j, $\epsilon_{ij} = \frac{1}{im(i,j)}$, where function $im(\cdot)$ is the importance measurement over the two elements s_i and s_j. Let (ϵ, g) and (k, m) be the spatial coordinates of s_i and s_j. The European distance is specifically considered, that is, $\epsilon_{ij} = 1/\sqrt{(\epsilon-k)^2+(g-m)^2}$.

We adopted an augmented multiplicative update method to solve the model (4). Specially, in the tensor factorization term, $\mathbf{A}_r$ and $\mathbf{B}_r$ are treated as a whole, while in the sparse regularization term we treat them independently. By embedding $\mathbf{U} = \mathbf{A}$ and $\mathbf{V} = \mathbf{B}$ in (4) to split the variables, the model of SSWNTF can be rewritten as

$$\begin{aligned}\min_{\mathbf{A},\mathbf{B},\mathbf{C}} &\left\|\chi - \sum_{r=1}^{R}\mathbf{A}_r\mathbf{B}_r^T\circ\mathbf{c}_r\right\|_F^2 + \frac{\delta}{2}\left\|\mathbf{A}\mathbf{B}^T - \mathbf{1}_{I\times J}\right\|_F^2 \\ &+\lambda\sum_{r=1}^{R}\left\|(\mathbf{W}_r^{spe}\mathbf{W}_r^{spa})\odot(\mathbf{A}_r\mathbf{B}_r^T)\right\|_1 + \frac{\mu}{2}(\|\mathbf{U}-\mathbf{A}\|_F^2 \\ &+\|\mathbf{V}-\mathbf{B}\|_F^2) \quad \text{s.t.}\mathbf{A},\mathbf{B},\mathbf{C}\geq 0\end{aligned} \tag{8}$$

where μ is a parameter for controlling the difference between the primal and the auxiliary variables. The optimization problem of each variable is split. Under the model in (4), the update rules are given by

$$\mathbf{A} \leftarrow \mathbf{A}.*(\mathbf{X}_{(1)}^T\mathbf{M}+\delta\mathbf{1}_{I\times J}\mathbf{B}+\mu\mathbf{U})./(\mathbf{A}\mathbf{M}^T\mathbf{M}+\delta\mathbf{A}\mathbf{B}^T\mathbf{B}+\mu\mathbf{A}) \tag{9}$$

where $\mathbf{X}_{(1)}$ denotes the mode-1 unfolding of χ and $\mathbf{M} = \mathbf{B}\bar{\odot}\mathbf{C}$ represents the partition-wise Kronecker product of matrix $\mathbf{B}$ and $\mathbf{C}$. The operands $.*$ and $./$ denote element-wise multiplication and division.

$$\mathbf{B} \leftarrow \mathbf{B}.*(\mathbf{X}_{(2)}^T\mathbf{M}+\delta\mathbf{1}_{I\times J}^T\mathbf{A}+\mu\mathbf{V})./(\mathbf{B}\mathbf{M}^T\mathbf{M}+\delta\mathbf{B}\mathbf{A}^T\mathbf{A}+\mu\mathbf{B}) \tag{10}$$

where $\mathbf{X}_{(2)}$ denotes the mode-2 unfolding of χ, $\mathbf{M} = \mathbf{C}\bar{\odot}\mathbf{A}$.

$$\mathbf{C} \leftarrow \mathbf{C}.*(\mathbf{X}_{(3)}^T\mathbf{M})./(\mathbf{C}\mathbf{M}^T\mathbf{M}) \tag{11}$$

Table 1. SAD of the unmixing methods under different noise level.

SNR(dB)	20	30	40
VCA	0.4295	0.4027	0.3819
NMF	0.4064	0.3872	0.3642
$L_{1/2}$-NMF	0.3926	0.3571	0.3314
MVNTF	0.3675	0.3265	0.3146
SSWNTF	**0.3378**	**0.3034**	**0.3001**

Table 2. RMSE of the considered unmixing methods under different noise levels.

SNR(dB)	20	30	40
VCA	0.1543	0.1245	0.1241
NMF	0.1399	0.1231	0.1224
$L_{1/2}$-NMF	0.1303	0.1205	0.1163
MVNTF	0.1237	0.1178	0.1078
SSWNTF	**0.1196**	**0.1093**	**0.0984**

where $\mathbf{X}_{(3)}$ denotes the mode-3 unfolding of χ, $\mathbf{M} = [(\mathbf{A}_1\odot\mathbf{B}_1)1_L\ldots(\mathbf{A}_R\odot\mathbf{B}_R)1_L]$

$$\mathbf{U}_r = \mathbf{U}_r.*(\mu\mathbf{A}_r)./(\mu\mathbf{U}_r+\lambda\mathbf{W}_r^{spe}\mathbf{W}_r^{spa}\mathbf{V}_r) \tag{12}$$

$$\mathbf{V}_r = \mathbf{V}_r.*(\mu\mathbf{B}_r)./[\mu\mathbf{V}_r+\lambda(\mathbf{W}_r^{spe}\mathbf{W}_r^{spa})^T\mathbf{V}_r] \tag{13}$$

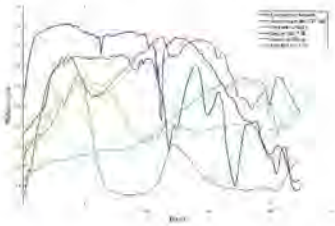

Fig. 1. Spectral signatures of six endmembers considered in our simulations.

4. EXPERIMENTAL RESULTS

In order to illustrate the performance of the proposed method, we compare the SSWNTF algorithm presented in this work with other advanced algorithms for hyperspectral unmixing, specifically with the vertex component analysis (VCA) method [3], the basic NMF [5] method, $L_{1/2}$-NMF [8] method, and the matrix-vector NMF (MV-NTF) [13] method.

We generated synthetic HSI data by adopting a similar procedure with regards to the one adopted in [13]. First, six endmember signatures that contain 224 spectral bands, with wavelengths ranging from 0.38 to 2.5 μm, are randomly chosen from the United States Geological Survey (USGS) library [1]. The spectral signatures of these six endmember signatures are shown in Fig. 1.

[1] Available online: https://speclab.cr.usgs.gov/spectral-lib.html

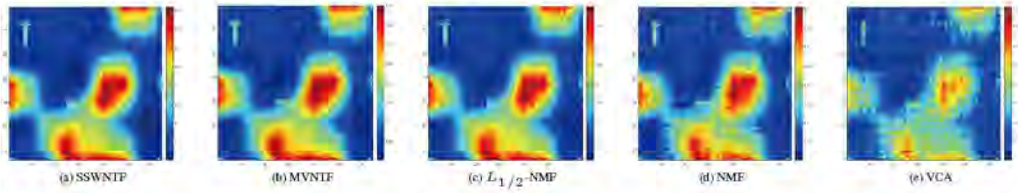

Fig. 2. Abundance maps obtained for the sixth endmember from the simulated data sets under SNR=20dB.

After generating the simulated data cubes, the zero-mean white Gaussian noise with SNR=20, 30, and 40dB are included in the experiments. The spectral angle distance (SAD) and the root mean square error (RMSE) were used to measure the unmixing performance. The $\mathbf{SAD}_r = \arccos\left(\frac{c_r^T \hat{c}_r}{\|c_r\|\|\hat{c}_r\|}\right)$ evaluates the dissimilarity of the r-th endmember signature c_r and its estimated signature $\hat{c}_r$. The $\mathbf{RMSE} = \left(\frac{1}{N}|\mathbf{E}_r - \hat{\mathbf{E}}_r|^2\right)^{\frac{1}{2}}$ measures the error between the real abundance map $\mathbf{E}_r$ of the r-th endmember and its estimated map $\hat{\mathbf{E}}_r$, where $N = I \times J$ is the number of pixels in the image. In our experiments, we use the average SAD of all endmembers and the average RMSE of all abundance maps to indicate the unmixing performance, which are defined as $\mathbf{SAD} = (1/R)\sum_{r=1}^{R} \mathbf{SAD}_r$ and $\mathbf{RMSE} = (1/R)\sum_{r=1}^{R} \mathbf{RMSE}_r$, respectively. The smaller the SAD and the RMSE, the more accurate the unmixing results. For all the considered algorithms, the input parameters have been carefully adjusted to achieve optimal performance. Besides, we use a random method to initialize $\mathbf{A}$,$\mathbf{B}$, $\mathbf{C}$, and all the tested methods are initialized with the same values.

Table 1 and Table 2 show the SAD and RMSE results obtained by different algorithms under all considered SNR levels. We can see that the proposed SSWNTF algorithm obtains better SAD and RMSE results than other algorithms in all cases, which indicates that the spectral-spatial weighted strategy can improve the unmixing performance. Fig. 2(a)-(e) show a graphical comparison of the considered unmixing algorithms for the simulated problem with SNR of 20dB, in which only the abundance map of endmember 6 is presented, as the abundance maps estimated for all endmembers exhibited similar behavior. It can be seem from Fig.2 that the results obtained by SSWNTF are better than those provided by other methods in the case of low SNR, which indicates that the inclusion of the spatial weighting factor in the NTF model can further promote the piecewise smoothness of the abundance map.

5. CONCLUSIONS AND FUTURE WORK

In this paper, we have introduced a new spectral-spatial weighted sparse nonnegative tensor factorization (SSWNTF) algorithm for blind unmixing of hyperspectral data. For the proposed SSWNTF algorithm, the spatial weighting factor is used to promote piecewise smoothness in abundance maps, while the spectral weighting factor is used to enforce the sparsity of the solution. The experimental results with simulated hyperspectral data reveal that the SSWNTF algorithm outperforms other state-of-the-art unmixing algorithms. Future work will focus on conducting additional experiments with real hyperspectral images.

6. REFERENCES

[1] J.M. Bioucas-Dias, A. Plaza, N. Dobigeon, M. Parente, Q. Du, P. Gader, and J. Chanussot, "Hyperspectral unmixing overview: Geometrical, statistical, and sparse regression-based approaches," *IEEE J. Sel. Topics Appl. Earth Observ. Remote Sens.*, vol. 5, no. 2, pp. 354–379, Apr. 2012.

[2] N. Keshava and J.F. Mustard, "Spectral unmixing," *IEEE Signal Process. Mag.*, vol. 19, no. 1, pp. 44–57, Jan. 2002.

[3] J.M. Nascimento and J.M. Bioucas-Dias, "Vertex component analysis: A fast algorithm to unmix hyperspectral data," *IEEE Trans. Geosci. Remote Sens.*, vol. 43, no. 4, pp. 898–910, 2005.

[4] M. Berman, H. Kiiveri, R. Lagerstrom, A. Ernst, R. Dunne, and J. F. Huntington, "Ice: a statistical approach to identifying endmembers in hyperspectral images," *IEEE Trans. Geosci. Remote Sens.*, vol. 42, no. 10, pp. 2085–2095, Oct 2004.

[5] D. D Lee and H. S. Seung, "Algorithms for non-negative matrix factorization," in *Proc. NIPS*, 2001, pp. 556–562.

[6] X. Xu, J. Li, S. Li, and A. Plaza, "Generalized morphological component analysis for hyperspectral unmixing," *IEEE Trans. Geosci. Remote Sens.*, 2019.

[7] L. Miao and H. Qi, "Endmember extraction from highly mixed data using minimum volume constrained nonnegative matrix factorization," *IEEE Trans. Geosci. Remote Sens.*, vol. 45, no. 3, pp. 765–777, Mar. 2007.

[8] Y. Qian, S. Jia, J. Zhou, and A. Robles-Kelly, "Hyperspectral unmixing via $l_{1/2}$ sparsity-constrained nonnegative matrix factorization," *IEEE Trans. Geosci. Remote Sens.*, vol. 49, no. 11, pp. 4282–4297, Nov. 2011.

[9] X. Lu, H. Wu, Y. Yuan, P. Yan, and X. Li, "Manifold regularized sparse nmf for hyperspectral unmixing," *IEEE Trans. Geosci. Remote Sens.*, vol. 51, no. 5, pp. 2815–2826, May 2013.

[10] W. He, H. Zhang, and L. Zhang, "Total variation regularized reweighted sparse nonnegative matrix factorization for hyperspectral unmixing," *IEEE Trans. Geosci. Remote Sens.*, vol. 55, no. 7, pp. 3909–3921, 2017.

[11] T. G Kolda and B. W Bader, "Tensor decompositions and applications," *SIAM review*, vol. 51, no. 3, pp. 455–500, 2009.

[12] F. Xiong, Y. Qian, J. Zhou, and Y. Tang, "Hyperspectral unmixing via total variation regularized nonnegative tensor factorization," *IEEE Trans. Geosci. Remote Sens.*, vol. 57, no. 4, pp. 2341–2357, 2018.

[13] Y. Qian, F. Xiong, S. Zeng, J. Zhou, and Y. Tang, "Matrix-vector nonnegative tensor factorization for blind unmixing of hyperspectral imagery," *IEEE Trans. Geosci. Remote Sens.*, vol. 55, no. 3, pp. 1776–1792, 2016.

[14] S. Zhang, J. Li, H. Li, C. Deng, and A. Plaza, "Spectral-spatial weighted sparse regression for hyperspectral image unmixing," *IEEE Trans. Geosci. Remote Sens.*, vol. 56, no. 6, pp. 3265–3276, 2018.

[15] R. Wang, H. C. Li, A. Pizurica, J. Li, A. Plaza, and W. J. Emery, "Hyperspectral unmixing using double reweighted sparse regression and total variation," *IEEE Geosci. Remote Sens. Lett.*, vol. 14, no. 7, pp. 1146–1150, Jul. 2017.